Original Research Article

Corrosion behavior of welded joints of X70 pipeline steel produced by high-frequency welding

Abstract: Corrosion behavior of welded joints of pipe steel category X70 produced by high-frequency welding, in different conditions, in which it is possible to initiate stress-corrosion cracking, hydrogen or sulfide cracking, is investigated. According to the results of electrochemical researches, the kinetic parameters of the cathode and anode processes on the surface of the welded joint of pipe in the investigated solutions are determined. Corrosion resistance of the welded joint HFW-pipe is similar to corrosion resistance of the base metal.

Key words: *pipe, high-frequency welding, corrosion, stress-corrosion cracking, corrosion potential*

Introduction.

It is well-known that pipes of big diameter from 530 to 1420 mm for pipelines are manufactured using arc welding under flux [1-3]. In this case the effectivity of such type of welding significantly decreasing with decreasing of the thick of pipe wall. Moreover, taking into the account the obligatory implementation of double-sided welding, the equipment for arc welding is considerably complicated, due to the need to transport flux inside the pipe. This contributed to the intensive development of high-frequency welding (HFW) method, primarily for small and medium diameter pipes. Up to date, in the world, with the HFW technology produces pipes of the categories X65 ... X80 with the diameter from 219 to 660 mm and wall thickness up to 25,4 mm. Despite the rapid development of this technology, at the present time in the scientific and technical literature there is virtually no information on the corrosion resistance of the welded joints of HFW-pipes.

The purpose of this work was to investigate the corrosion behavior of welded joints of HFW-pipes, on the example of Ø508.0 × 8.7 mm pipes from a steel of category X70, in the conditions where initiation of stress-corrosion cracking, hydrogen or sulfide cracking is possible. This researches were conducted in two directions. The first, were evaluation of electrochemical properties in the environments of different aggressiveness. The second, is corrosion resistance in hydrogen sulfide solutions. Also, took into the account the peculiarities of the design of the connections of HFW-pipes, that determined by the implementing of the pressure welding, and also the presence of heat treatment in a mode close to normalization, including significantly less, in comparison to the arc processes, chemical and structural heterogeneity.

34 **Materials and methods.**

35 **The chemical composition** of the investigated material was determined by the spectral method on

36 the device "Spectrovak-1000" produced by the company "Baird". The chemical composition of rolling

37 steel is shown in Table 1.

38 **Table 1** - Chemical composition of the base metal of HFW-pipes

Chemical composition, wt-% max											
C	*Si*	*Mn*	*P*	*S*	*V*	*Nb*	*Ti*	*Ni*	*Cr*	*Al*	*Cu*
0,08	0,22	1,34	0,014	0,006	0,040	0,06	0,014	0,19	0,22	0,037	0,02

39 **Metallographic research** of the microstructure were carried out on the microscope "Neofot-21"

40 after the microsection etching in the nital.

41 **Electrochemical measurements**.

42 The evaluation of the corrosion resistance of the welded joint of the HFW-pipe in various media

43 were carried out by the method of polarization curves. As a rule, from the experience of operating oil and

44 gas pipelines, stress-corrosion cracking occurs in the environment with a hydrogen index close to neutral

45 [4-6]. Thereby, the tests were carried out in three solutions with a hydrogen index in the range from 5.4 up

46 to 8.4: 3% NaCl з pH 6,8 [4] (solution №1); 0,037 g/l KCl+0,559 g/l NaHCO$_3$+0,008 g/l CaCl$_2$+0,089 g/l

47 MgSO$_4$·7H$_2$O, pH 8,2-8,4 [5-6] (solution №2); 1,92 g/l HCOOH + 54,5 g/l HCOONa + 10 g/l KCNS, pH

48 5,4 [7] (solution №3).

49 Electrochemical researches were carried out on the microsection of the welded joints of the HFW-

50 pipe Ø508,0 × 8,7 mm in the size of 50×20×8,7 mm, with the fusion zone in the middle. Before research,

51 samples were sanded with sandpaper of different grain sizes from 320 to 1000, then washed with running

52 and distilled water and rubbed with alcohol. On the surface of the welded joint area of 5 mm^2 installed

53 clamping electrochemical cell, the other surface was protected by an insulating coating. Measurement was

54 carried out according to the three electrode scheme: working electrode (WE) - basic metal and weld joint;

55 auxiliary electrode (AE) - platinum, comparison electrode (CE) - chlorine-silver electrode. The

56 polarization curves were measured in dynamical mode at the speed of potential sweep of 0.0005 V/s. The

57 polarization range from the corrosion potential was 1.5 V to the cathode side and 2.0 V to the anode. The

58 time for measuring the potential of the corrosion potential of the working sample was 60 minutes, after

59 which the potential for scanning was switched on. From the received polarization curves were determined

60 corrosion potential, the current in the region of active anode dissolution for the potential -0.5 V ($i_{-0.5 V}$),

61 the Tafel slope of the initial part of the anode curve (b_a), the limiting diffusion current (i_d) and the

62 potential for initiating the release of hydrogen (E_{H_2}). In analyzing the influence of the protective potential

63 on the corrosion of the surface of the pipe under the protective cover, it is proposed to determine the

64 current density of the cathode protection (j_{cp}) and compare it with the density of the limiting current of

65 oxygen recovery (j_{O_2}) [8]. If the ratio of currents is less than 1, corrosion of the pipe wall in the coating

66 defect is possible; if the ratio of currents is in the range from 1 to 3 - protective effect is achieved. Further

67 increase in the current density of the cathode protection does not lead to a significant reduction in the rate

68 of corrosion, but is accompanied by a sharp increase in the volume of hydrogen which is formed during

69 the decomposition of the electrolyte.

70 **Investigation of the resistance of the welded joint of HFW-pipes against hydrogen cracking**

71 **and hydrogen sulfide corrosion cracking.**

72 According to the requirements of ANSI / API specification 5L [9], corrosion researches are carried

73 out, by the results of which corrosion rate of the metal in an environment that containing hydrogen sulfide,

74 as well as its resistance to hydrogen cracking (HC) and hydrogen sulfide cracking (HSC) is determined.

75 Tests for resistance to HC were conducted in accordance with NACE TM 0284-2003 [10] for 96 hours.

76 After the tests, each sample was cut into 3 equal parts. Metallographic specimen was made, and the rate of

77 total corrosion, Crack Length Ratio (CLR), Crack Thickness Ratio (CTR), which, accordingly, should not

78 exceed 0.5 mm/year, were determined, CLR-6 % and CTR - 3%.

79
$$CLR = \frac{\sum a}{W} \cdot 100 \ \%$$

80
$$CLR = \frac{\sum b}{T} \cdot 100 \ \% \ .$$

81 where a - length crack, b - thickness crack, W - section width, T - test specimen thickness.

82 For tests of resistance to hydrogen sulfide cracking (HSC), the samples were made in such a way

83 that one of the surfaces is located at the minimum possible distance from the inner surface of the pipe.

84 Tests were conducted into the accordance to NACE TM 0177-2005 (method B, ISO 7539-2-89) for 720

85 hours [11]. The load level was equal. The criterion of resistance to HSC is the absence of cracks.

86 **Results and discussion.**

87 The microstructure of the fusion zone of the HFW pipe Ø508.0 × 8.7 mm from steel of category

88 X70 is shown in Figure 1. The fusion line represents a distinct continuous carbon-free light band. Due to

89 the local thermal treatment of coarse-grained lamellar or needle structure that formed after welding in the

90 zone of thermal influence, transforms into fine-grained ferrite-perlite. The amount of perlite component in
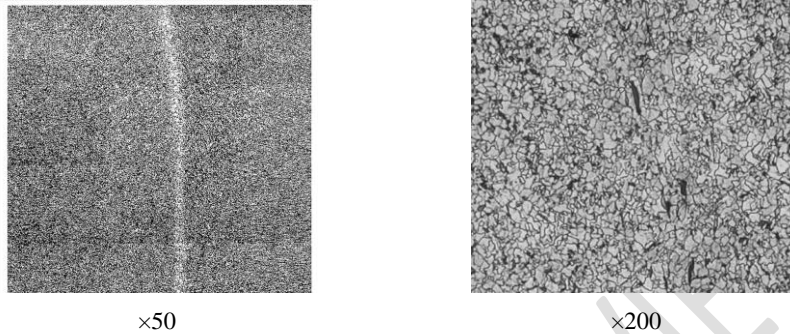91 the structure is determined by the carbon content of the steel.

| ×50 | ×200 |

Figure 1 - Microstructure of the fusion zone of the HFW-pipe welded joint Ø508.0 × 8.7 mm
from steel category X70 after etching in the nital

92   The microstructure of the base metal and the heat affected zone of the pipe is a fine-grained ferrite-
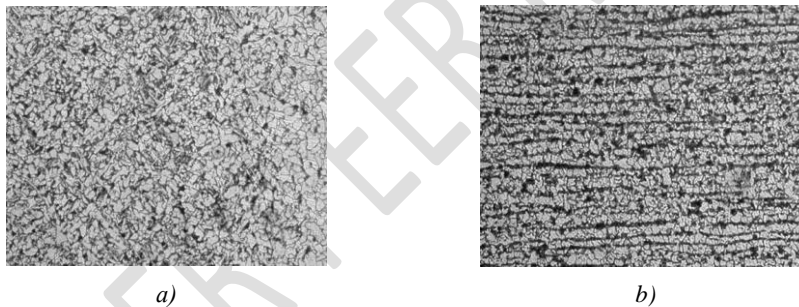93 perlite mixture with enough highlighted strips (Figure 2).

| *a)* | *b)* |

Figure 2 – Microstructure of the base metal of the HFW-pipe Ø508,0 × 8,7 mm from steel
category X70, heat affected zone (a) and base metal (b) after etching in 4% nital, × 200

94   Figures 3, 4 and 5 shows the dynamics of changes in the corrosion potential (a) and the
95 polarization curves (b) of the base metal (BM) and the welding joint (WJ) of the HFW-pipe in solutions №
96 1, № 2 and № 3, respectively. As can be seen from the curves presented Fig. 3a, the corrosion potentials
97 on BM and WJ are close in value and are -0.570 V and -0.584 V respectively. The behavior of the anode
98 and cathode curves of the two welded zones is similar Fig. 3b. The numerical values of the
99 electrochemical parameters of the cathode and anode processes, that was determined graphically from Fig.
100 3b, is shown in Table 2. From the corrosion potential up to 0.5 V for both zones in this solution, is
101 characterized a wide area of active dissolution. There is a slightly smaller angle of the Tafel slope of the
102 starting zone of the anode curve of WJ zone in comparison the BM, which indicates a higher rate of anode

103 dissolution under the same conditions. For potentials larger than -0.25 V, the deceleration of the anode
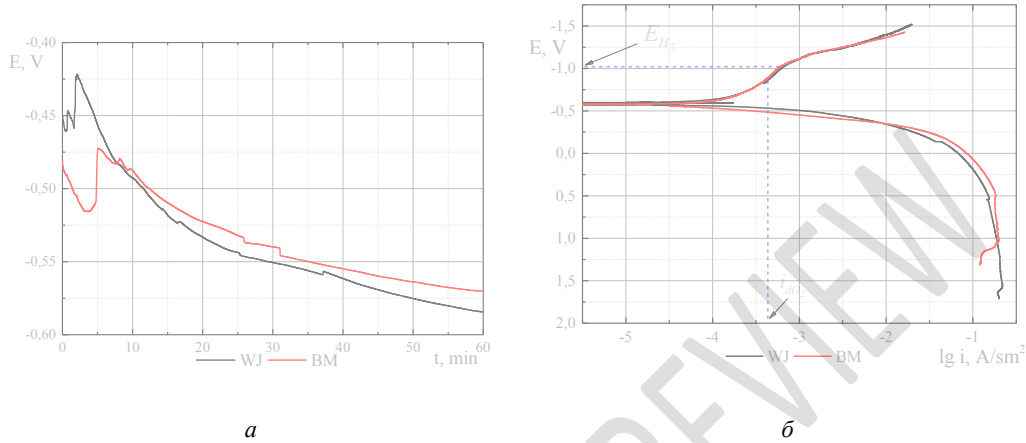104 dissolution was observed due to passivation of the surface of the sample.

a   *б*

Figure 3 - Changes in corrosion potential in time (a) and the polarization curves (b) BM and WJ of the
sample of the HFW-pipe in solution №1.

105   In the solution №2, BM is characterized by a sharp shift of the corrosion potential in the region of
106 negative values from -0.455 V that stabilizes after 60 minutes at -0.641 V, and on the WJ were shifted
107 smoothly from -0.490 V, and stabilizes at -0.596 V, Fig. 4a. This difference in potentials is significant, but
108 considering the much smaller area of the WJ as compared to the BM, it does not pose any danger in terms
109 of the development of local corrosion processes. The area of active dissolution is long enough for both
110 zones - from the potential of corrosion to the potential is about -0.25 V, above which there is a slowing
111 down of the anode process due to the surface shielding by products of corrosion. The Tafel's angles of
112 slope of the initial regions of the anode curves indicate a higher rate of dissolution of the BM in
113 comparison with the WJ.

114   In solution № 3, the dynamics of the change in corrosion potentials within 60 minutes is
115 characterized by a slight displacement in the region of positive values for both on the BM and the WJ,
116 varying from -0.632 V up to -0.604 V and -0.636 V up to -0.622 V, respectively. The electrochemical
117 characteristics of the anode and cathode processes on the BM and the WJ are shown in Table 2. The
118 analysis of the course of the anode curves shows that the rate of dissolution of the WJ at the potential -0.5
119 V is almost 6 times higher than the BM (Table 2). Both zones are characterized by the area of active
120 dissolution: for the BM in the range -0.543 ... -0.03 V; for the WJ - -0.588 ... 0.25 V.
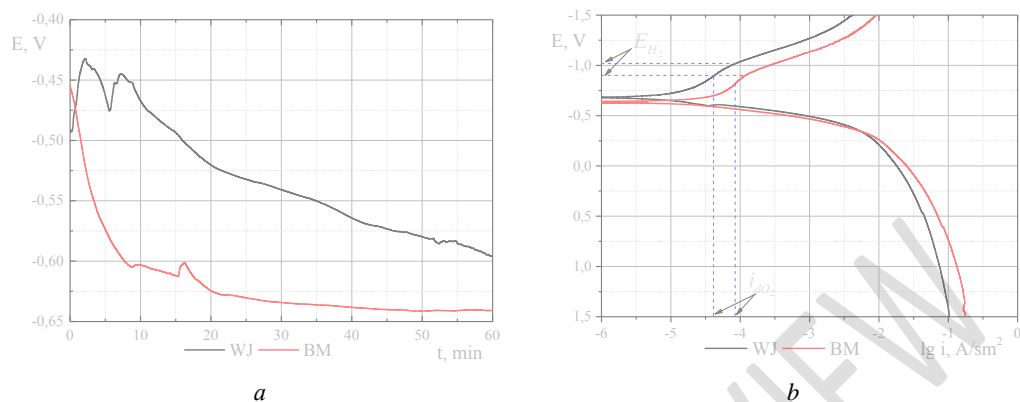
Comment [LK7]: delete

Figure 4 - Changes in corrosion potential in time (a) and the polarization curves (b) of the BM and the WJ of the sample of the HFW-pipe in solution №2
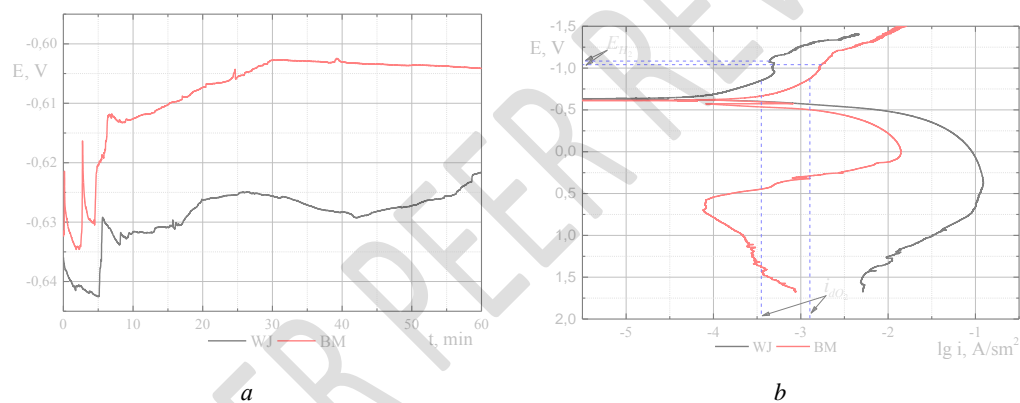

Figure 5 - Changes in corrosion potential in time (a) and polarization curves (b) of the BM and the WJ of the sample of the HFW-pipe in solution №3

121   The analysis of the ratio of currents j_{cp}/j_{O_2} for the region of the WJ and the BM were conducted

122   in order to determine the possible formation on the surface of the pipe under peeling coating of local areas

123   with different electrochemical activity. The results of the analysis are shown in Table 2.

124   From the analysis of experimental data it can be concluded that in the range of protective potentials (from

125   -0.85 V up to -1.15 V relative to copper-sulfate electrode comparison, which corresponds the value from

126   -0.75 V to -1.05 V relative to the chlorine-silver electrode comparison), the ratio of currents j_{cp}/j_{O_2} in

127   solutions № 1-3, both on the BM and on metal of the WJ is more than 1 by the polarization potential,

128   which is approaching the maximum protective value. Such conditions contribute to the decomposition of

129 the electrolyte with hydrogen release. But it should be noted that the ratio of currents j_{cp}/j_{o_2} for the BM

130 and the WJ practically does not differ. This indicates that when working under the conditions of cathodic

131 protection of hydrogen absorption of the weld and base metal is not expected.

132   The results of the study of the resistance of the welded joint of the HFW-pipe to the HC and the

133 HSC are given in Table 3.

134   **Table 2** - Electrochemical characteristics of different zones of the HFW-pipes in solutions №1-3

Solution	Zone	Electrochemical characteristics				Currents of cathode protection, A/m²		Ratio j_{cp}/j_{o_2}	
		anode		cathode					
		$i_{-0.5\,B}$, A/м²	b_a, B	i_d, A/м²	E_{H_2}, B	for cathode potentials -0,75 V	for cathode potentials -1,05 V	for cathode potentials -0,75 V	for cathode potentials -1,05 V
№1	BM	$1,1\times10^{-3}$	0,069	0,0007	-1,03	$2,8\times10^{-4}$	$7,6\times10^{-4}$	0,4	1,08
	WJ	$3,1\times10^{-4}$	0,054	0,0007	-1,03	$2,8\times10^{-4}$	$7,6\times10^{-4}$	0,4	1,08
№2	BM	$1,2\times10^{-4}$	0,074	$8,2\times10^{-5}$	-0,94	$4,5\times10^{-5}$	$2,6\times10^{-4}$	0,5	3,2
	WJ	$8,1\times10^{-4}$	0,087	$3,8\times10^{-5}$	-1,0	$1,5\times10^{-5}$	$1,1\times10^{-4}$	0,4	2,9
№3	BM	$1,2\times10^{-3}$	0,057	$1,5\times10^{-3}$	-1,2	$7,1\times10^{-4}$	$1,8\times10^{-3}$	0,5	1,2
	WJ	$6,8\times10^{-3}$	0,069	$5,0\times10^{-4}$	-1,2	$2,5\times10^{-4}$	$4,9\times10^{-4}$	0,5	1,0

135   **Table 3** - Indicators of corrosion resistance of the BM and the WJ metal of HFW-pipes

Zone	Indicators of corrosion resistance			
	Corrosion rate, mm/year	HC		HSC at $0,7\sigma_{0,2}$
		CLR, %	CTR, %	
BM	0,5	3,2-3,7	2,0-2,3	Cracks are not detected
WJ	-	0,0	0,0	Cracks are not detected

136
137
138
139
140
141
142
143
144

The results obtained in Table 4 show that the welded joint of the HFW-pipe is resistant to HC and HSC by the determined parameters (corrosion rate,

145 CLR, CTR, HSC resistance at 0.7σ 0.2 for 720 hours).

146 **Conclusions**

147 1. The mechanism of anodic dissolution of both the base metal and the welding joint is controlled by

148 diffusion of oxygen, which is confirmed by the values of the Constants of Tafel (from 0.054 V to 0.087

V). Differences in the values of the observed Tafel's slopes, indicate a greater or lesser speed of this process. Such anode behavior indicates that the corrosion resistance of the welded joints of the HFW-pipes in general is similar to the corrosion resistance of the base metal.

2. The potential for the initiation of hydrogen release in the range of pH from 5.4 to 8.2 is approximately similar for the base metal and for the weld joint.

3. In the range of protective potentials in solutions of different aggressiveness, the ratio of the current of cathode protection to the boundary diffusion current $j_{cp} \big/ j_{O_2}$ for the base metal and the weld joint does not differ. Thus, in the conditions of cathodic protection, flooding of the base metal and the weld is not expected.

Summing up the above, it can be argued that when operation a pipeline constructed using high-frequency welding technology under pressure in the conditions of cathodic protection, the resistance of welded joints to stress-corrosion cracking will depend only on the protective properties of the insulating coating.

References

1. Zeng Huilin, Wang Changjiang, Yang Xuemei, Wang Xinsheng, Liu Ran. Automatic welding technologies for long-distance pipelines by use of all-position self-shielded flux cored wires//Natural Gas Industry B. – Vol. 1, Issue 1, October 2014, Pages 113-118.

2. Yongchang Liu, Yi Shao, Chenxi Liu, Yan Chen, Dantian Zhang. Microstructure Evolution of HSLA Pipeline Steels after Hot Uniaxial Compression//Materials (Basel). 2016 Sep; 9(9): 721.

3. Satish Kumar Sharma, Sachin Maheshwari. A review on welding of high strength oil and gas pipeline steels//Journal of Natural Gas Science and Engineering. – Vol. 38, February 2017, Pages 203-217February 2017, Pages 203-217.

4. Technical challenges of heavy wall HFW-pipe production for Bord gáis éireann pipeline project. /Paul O'Dwyer, Athanasios Tazedakis, Peter Boothby/ Proceedings of the 8th International Pipeline Conference IPC2010. September 27-October 1, 2010, Calgary, Alberta, Canada. IPC 2010-31293

5. Szklarska-Smialowska K Z., Xia Z., Rebak R.B. Technical note: stress corrosion cracking of X-52 carbon steel in dilute aqueous solutions/ Corrosion. –Vol.50. – No.5. – 1994. – P.334-338.

6. Jinheng Luo, Sheji Luo, Lifeng Li, Liang Zhang, Gang Wu, Lixia Zhu. Stress corrosion cracking behavior of X90 pipeline steel and its weld joint at different applied potentials in near-neutral solutions/Natural Gas Industry B.-Available online 16 March 2019, open access. https://www.sciencedirect.com/science/article/pii/S2352854019300270

180   7.   Lubenskij A.P.; Lubenskij S.A.; CHeburahtin N.A.; Antonov V.G. Lubenskij. Sostav dlya
181 provedeniya ispytanij na stojkost' trubnyh stalej k korrozionnomu rastreskivaniyu pod napryazheniem.
182 Patent RF № 2082154. – Zayavl. 12.07.1994. – Opubl. 20.06.1997.

183   8.   Hizhnyakov   V.I.   Korrozionnoe   rastreskivanie   napryazhenno-deformirovannyh
184 truboprovodov pri transporte nefti i gaza / V.I. Hizhnyakov, YU. A. Kudashkin, M.V. Hizhnyakov,
185 A.V. ZHilin. // Izvestiya Tomskogo politekhnicheskogo universiteta. Himiya. – 2011. – T. 319. – № 3. –
186 S. 84-89.

187   9.   ANSI/APISpec.5L:2007/ISO 3183:2007. Specification for Line Pipe. Petroleum and natural
188 gas industries—Steel pipe for pipeline transportation systems.

189   10.   NACE TM 0284-2003 Standard Test Method Evaluation of Pipeline and Pressure Vessel
190 Steels for Resistance to Hydrogen-Induced Cracking

191   11.   NACE TM 0177-2005 Standard Test Method Laboratory Testing of Metals for Resistance to
192 Sulfide Stress Cracking and Stress Corrosion Cracking in H2S Environments
193